Polarization fields in (Zn,Cd)O/ZnO quantum well structures

S. Kalusniak, S. Sadofev, J. Puls, H. J. Wünsche, and F. Henneberger*
Institut für Physik, Humboldt-Universität zu Berlin, D-12489 Berlin, Germany
(Received 7 December 2007; published 26 March 2008)

The presence of polarization-induced electric fields of some 10^8 V/m in (Zn,Cd)O/ZnO quantum well structures is uncovered by a low-energy shift of the photoluminescence of several 100 meV as well as a dramatic increase of the lifetime from the sub-ns to the 100 μs time scale when the well width increases from 1.2 to 5.4 nm. Effective screening of these fields by photogenerated carriers occurs already at moderate optical excitation in the 10 kW/cm^2 range.

DOI: 10.1103/PhysRevB.77.113312 PACS number(s): 78.67.De, 78.66.Hf, 73.21.Fg

The ternary ZnCdO is a material with considerable potential for optoelectronic applications as it can cover in principle band-gaps extending from the ultraviolet to the near infrared spectral range. An obstacle that had to be overcome is phase separation forced by the different crystalline structure of the binaries, wurtzite for ZnO and rocksalt for CdO. Epitaxial growth far from thermal equilibrium has made it possible to alloy ZnO with CdO in strict wurtzite phase beyond concentrations of 30% (Ref. 1–3) and to fabricate well-defined (Zn,Cd)O/ZnO quantum well (QW) structures.[2] Indeed, visible-wavelength laser action of appropriately designed specimen reaching the green wavelength range has been accomplished recently.[4] Typically, when using standard substrates, the growth direction of the QW structures is along the polar *c* axis of the wurtzite lattice. As a consequence, built-in electric fields originating from spontaneous as well as piezoelectric polarizations are generated.[5] The impact of such fields on the optical properties of group-III nitride QW structures has been extensively studied in the past (see, e.g. Refs. 6–8). When aiming at light-emitting devices, screening of the polarization charges by the injected carriers is of direct practical relevance. On the other hand, polarization fields can induce a two-dimensional carrier gas at the heterointerfaces that can be exploited for high-speed electronic applications. Theoretical work has predicted similarly huge polarization effects for ZnO/CdO as for nitride-based heterostructures,[9] however, to the best of our knowledge, no experimental data are available so far.

The set of single quantum well (SQW) structures used in this study is grown by radical-source molecular beam epitaxy on *a*-plane sapphire. The ZnCdO SQW is embedded between a 500-nm-thick ZnO buffer and a 30-nm-thick ZnO cap layer. The Cd concentration ($x=0.06-0.22$) and well width ($d=1.2-5.4$ nm) are determined from the specular beam intensity oscillations in reflection high-energy electron diffraction. While *d* is very accurately known, the relative error in *x* is about 5–10 % as it follows from a comparison with the composition of reference epilayers elaborated by energy-dispersive x-ray analysis. For more details of the growth process see Refs. 2 and 4. The low-density photoluminescence (PL) is excited by the frequency tripled output of a Nd:YVO_4 laser emitting 13 ps long pulses at a repetition rate of 80.6 MHz. Time-integrated spectra are recorded by a 1530-C/CVU 1024S EG&G CCD detector in conjunction with a 0.5 m focal-length monochromator. Time-resolved transients are excited by frequency doubled 2 ps/80.6 MHz pulses of a DCM dye laser and detected with a microchannel plate photomultiplier (MCP) and a time-correlated photon counting system. When needed, the repetition rate is lowered by an acousto-optical modulator. PL data at higher excitation intensities in time-integrated mode are acquired by an excimer laser pumped dye laser with a pulse duration of 20 ns and a repetition rate of 10 Hz. Time-resolved measurements in this regime are performed with 0.5 ns pulses of a N_2-laser using for detection a MCP and a digital oscilloscope. In all measurements the excitation (330 to 355 nm) is above the ZnO band gap and the sample temperature is 5 K.

Figure 1 systematizes steady-state PL data for the low-density regime. As depicted in Fig. 1(a) for a Cd concentration of $x=0.11$, the PL spectrum of the SQW structures consists of features from ZnO and the spectrally broader well emission situated on the low-energy side. Though the excited ZnO volume is at least one order of magnitude larger, the total yield of the low-energy PL is clearly stronger signifying efficient carrier capture by the SQW. The position of the well PL undergoes a huge low-energy shift of about 0.8 eV when the well width increases from 1.2 to 5.4 nm. As seen from the plot in Fig. 1(b), the shift is in good approximation a linear function of *d*. The same holds true when the PL position is plotted versus the Cd concentration at fixed well width [Fig. 1(c)], albeit a weak nonlinearity is indicated at higher *x*. The time-resolved PL transients represented in Fig. 2 demonstrate that the low-energy shift of the well PL is accompanied with a dramatic slow-down of the PL decay from about 500 ps up to the 100 μs range. The transients are nonexponential reflecting that the states behind the PL are not homogeneously broadened. Nonexponential PL decay is generally observed in heterostructures with strong polarization fields and has been attributed to a rather complex localization dynamics or a time shift of the transition energy.[7,8] Using a stretched exponential function $I(t)/I(0)=\exp(-t^\kappa/\tau^\kappa)$, the characteristic lifetime is determined from the area under the transients $\tau_{\mathrm{eff}}=\int_0^\infty dt\, I(t)/I(0)=\Gamma(1/\kappa)\tau/\kappa$. A striking observation in this context is that the yield of the wide SQW in Fig. 1(a) is only reduced by a factor of 1.5 relative to the 1.5 nm structure. That is, despite the extremely long lifetime, nonradiative processes are not substantially enhanced. For wider SQWs, as shown in Fig. 3, increase of the excitation intensity induces a high-energy shift of the well PL of several 100 meV. The shifts sets off already under steady-state excitation, but is much stronger

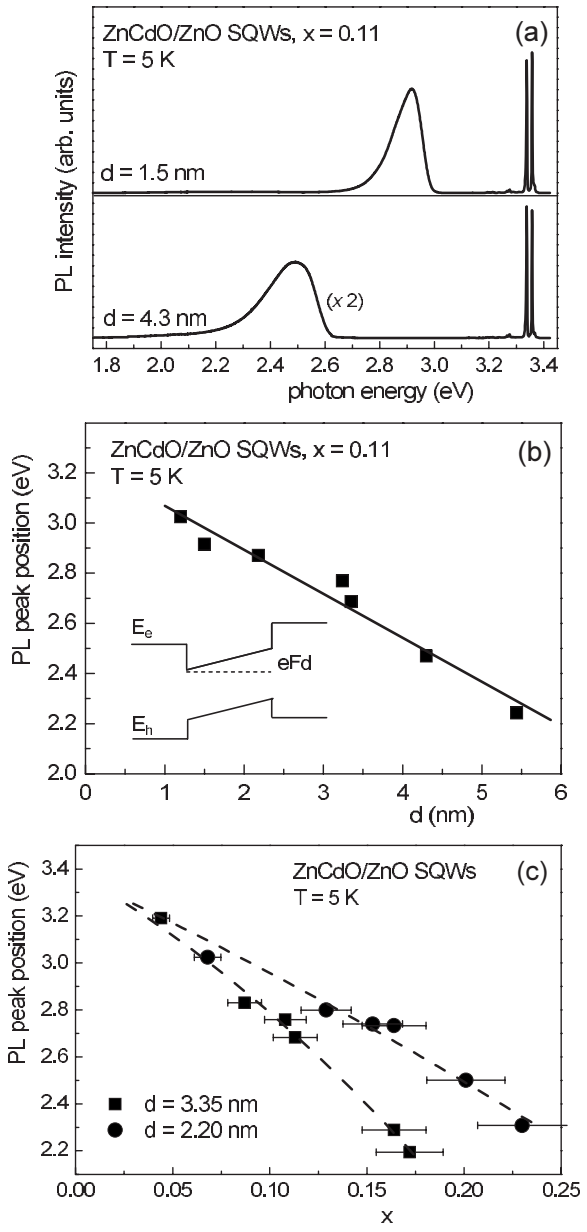

FIG. 1. PL data of (Zn,Cd)O/ZnO SQW structures. (a) Overview spectra of two structures with the same Cd concentration $x=0.11$ but different well width of $d=1.5$ and 4.3 nm, respectively. (b) PL peak energy versus well width for $x=0.11$. The line represents the slope given by the potential drop across the SQW $e\Delta\phi=1.75\times10^8$ eV/m as shown in the inset. (c) PL peak energy versus Cd concentration at fixed well width of $d=2.2$ and 3.35 nm, respectively. The dashed curves are to guide the eye. The excitation intensity is (a) $I_{exc}=500$ mW/cm^2 and (b) and (c) 10 mW/cm^2.

under pulsed pumping starting at about 10 kW/cm^2. No saturation is found up to excitation levels of 1 MW/cm^2. In parallel, the PL decay speeds up by orders of magnitude and reaches the sub-ns time scale. The decay transients of the 3.2 and 4.3 nm SQWs can be hardly separated from the instrumental response to the 500 ps excitation pulses (right-hand side inset of Fig. 2).

The above observations consistently evidence the presence of very strong polarization fields. The almost linear

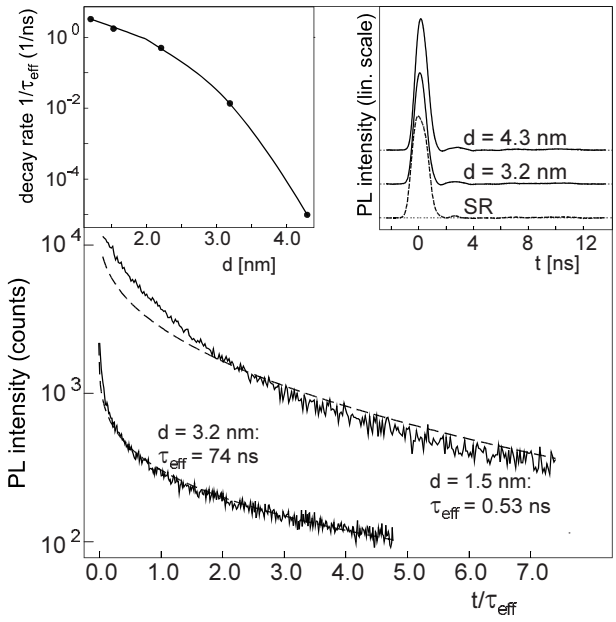

FIG. 2. Time-resolved PL data of (Zn,Cd)O/ZnO SQW structures. Main panel: Exemplary PL transients plotted in units of characteristic time τ_{eff} (see text). Left-hand inset: Inverse lifetime versus well width extracted from the transients by using a stretched exponential decay function as shown by the dashed curves in the main panel ($x=0.11$). Right-hand side inset: Transients taken at the PL peak in the high density regime in comparison with the system response (SR).

dependence of the optical transition energy on the well width as well as on the Cd concentration is fully confirmative of a high-field regime where the dominant energy contribution is given by the potential drop across the well $e\Delta\phi=eF(x)d$. Therefore, irrespective of the band structure details, the built-in electric field can be directly estimated from the experimental data providing $F/x=(1.6\pm0.2)\times10^9$ V/m [Fig. 1(b)]. This value is quite similar to the InN/GaN heterosystem,[6–8] but roughly a factor of five larger than data reported for ZnO/ZnMgO.[10] The field originates from the spontaneous polarization difference at the (Zn,Cd)O/ZnO interface and the strain-induced piezoelectric polarization in ZnCdO, both expected to increase linearly in lowest order with the Cd concentration. The determination of the polarization from the field is hampered by the lack of data for the dielectric constant of wurtzite CdO. Use of the values of ZnO ($\epsilon=8.75$) or rocksalt CdO ($\epsilon=21.9$) yields a range $P/x=(0.12-0.31)$ C/m^2 for the total polarization discontinuity which compares reasonably well with theoretical calculations predicting $P(x=1)=0.24$ C/m^2.[9] An estimation of the composition dependence of the piezoelectric and elastic strain constants from the slight nonlinearity in Fig. 2(c) with acceptable accuracy is questionable for the same reason.

The carriers generated by optical excitation screen the polarization fields. This is clearly manifested experimentally by the high-energy shift of the PL features as well as the shortening of the lifetime signifying recovery of strong overlap between electron and hole wave function. In order to understand the scenario in more detail, the system of the coupled Schrödinger and Poisson equations,

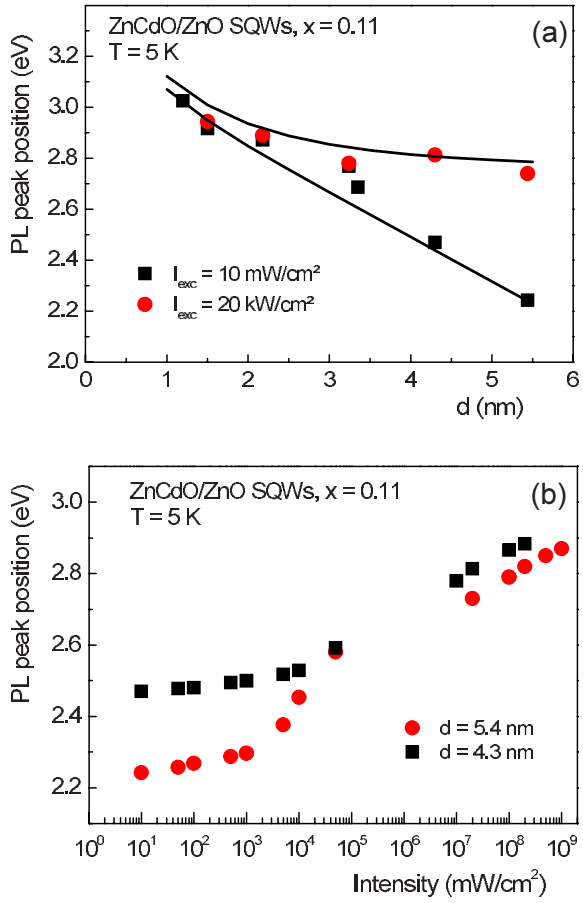

FIG. 3. (Color online) Effect of optical excitation on the PL from (Zn,Cd)O/ZnO SQWs. (a) Position of the dominant PL feature at low (squares, black) and high (circles, red/gray) excitation versus well width (x=0.11). The lines are calculated energies for wells with (lower) and without (upper) polarization field. For details see text. (b) Peak position versus excitation intensity for structures with x=0.11, d=4.3 nm (squares, black), and 5.4 nm (circles, red/gray).

$$\left[-\frac{\hbar^2}{2m_\alpha}\frac{\partial^2}{\partial z^2}+E_\alpha(z)+e_\alpha\phi(z)\right]\psi_{\alpha i}(z)=E_{\alpha i}\psi_{\alpha i}(z), \quad (1)$$

$$-\frac{\partial^2}{\partial z^2}\phi(z)=F[\delta(z-d)-\delta(z)]+\sum_\alpha\frac{e_\alpha n_\alpha(z)}{\epsilon_0\epsilon}, \quad (2)$$

$$n_\alpha(z)=N_\alpha\sum_i|\psi_{\alpha i}(z)|^2\ln\left[1+\exp\frac{\mu_\alpha-E_{\alpha i}}{k_BT}\right], \quad (3)$$

is solved numerically with boundary conditions $\phi'(\pm\infty)=0$ (charge neutrality) for the electrostatic potential. The index $\alpha=e,h$ refers to electron or hole, while i enumerates the quantum-confined states of the respective carrier type with mass m_α and chemical potential μ_α ($N_\alpha=\nu_\alpha m_\alpha k_BT/\pi\hbar^2$, $\nu_e=1$, $\nu_h=2$). A quantitative comparison with the experimental PL energies requires knowledge of the discontinuities of the band edges E_α which are not precisely known. For the excitonic band gap of wurtzite ZnCdO, quite conflicting relations have been put forward so far.[11,12] Photoelectron spectroscopy has provided a relative bandedge offset of $E_h/E_e=36/64$ for a composition of $x=0.05$.[13] Further uncertainties result from the carrier masses and localization effects. In addition, the theoretical model ignores the electron-hole Coulomb interaction and assumes rectangularly shaped wells. However, all these factors drop behind the huge field-induced energy changes in wider wells at sufficiently high Cd concentrations making an analysis in the above frame meaningful.

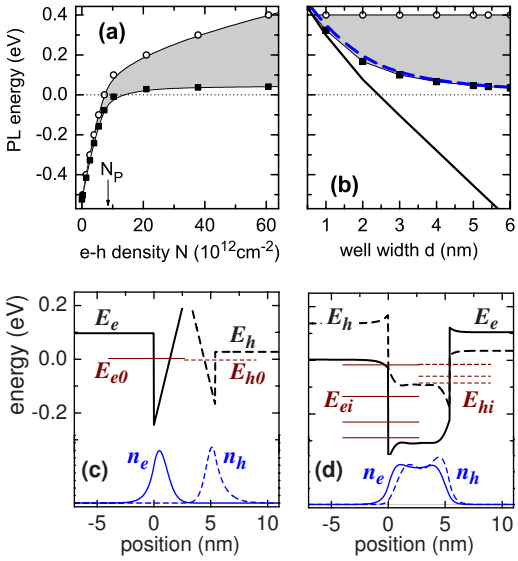

FIG. 4. (Color online) Screening scenario calculated by a self-consistent numerical solution of the Schrödinger-Poisson equations. (a) Ground-state transition energy E_{00} (squares) and chemical potential μ (circles) versus density N of photoexcited carriers. The energy origin is defined by the bulk energy-gap of the well material. (b) Ground-state transition energy versus well width without excitation (solid black) and under high excitation (squares) with μ =0.4 eV (circles). For comparison the dashed (blue/dark gray) curve represents E_{00} at zero field and no excitation. (c) and (d) Band diagrams E_α, particle densities n_α, and occupied subband levels $E_{\alpha i}$ for electrons (solid) and holes (dashed). Energies are measured relative to the respective chemical potential μ_α. Densities are in arbitrary units. Parameters: (c) ϵ=8.75, d=5.4 nm, $F=1.75\times10^8$ V/m, $N=10^8$ cm^{-2} and (d) $N=6\times10^{13}$ cm^{-2}.

In a first test, ground-state transition energies of the unexcited well ($n_e=n_h=0$) are calculated with and without the experimentally determined polarization field ($\phi=0$ or $\phi=Fz$ inside the well). When using the 36/64 offset and the ZnO masses ($m_e=0.28m_0$ and $m_h=0.59m_0$), one obtains a reasonably good fit to the PL positions in Fig. 3 using a bandgap $E_g(0.11)=2.9$ eV and subtracting from the calculated ground-state transition energy $E_{00}=E_{e0}+E_{h0}$ a constant value of 160 meV comprising both localization and exciton binding energy. Such assumption, also used for explaining findings for InGaN/GaN,[8] is justified by the fact that the PL linewidth changes only smoothly across the sample set. In addition, a possible increase of the localization energy will be at least partially compensated by a decrease of the exciton binding energy for SQWs with strong polarization field.

The results of the full numerical solution of equations (1)–(3) are summarized in Fig. 4. The sheet density

$$N = \int_{-\infty}^{\infty} dz\, n_{\alpha}(z) \tag{4}$$

of photoexcited carriers (or the total chemical potential $\mu = \mu_e + \mu_h$) is the parameter determining the excitation level in the calculations. The plots in Fig. 4(a) show that E_{00} shifts initially steeply to higher energies, but approaches a saturation level when N exceeds the sheet density $N_p = \epsilon\epsilon_0 F/e$ of polarization charges. At low densities before saturation, there is only one bound state for both electron and hole. The wavefunctions are located in the narrow triangular potential dips at the well edges, their overlap is thus very small [Fig. 4(c)], and E_{00} undergoes the anticipated low-energy drop as a function of the well width [Fig. 4(b)]. At high densities ($N > N_p$), the polarization charges become rapidly screened. The screening length is less than 1 nm so that a flat-band situation with several occupied subbands is established [Fig. 4(d)]. Figure 4(b) shows that E_{00} at high densities resembles indeed very well the energy of a fictive SQW with no polarization field under low-excitation. All these results are in very good qualitative agreement with the experimental findings.

In conclusion, (Zn,Cd)O/ZnO QW structures exhibit polarization fields similarly huge as known for III-nitride systems. For light-emitting applications, the recovery of flat-band conditions under carrier injection is an essential point. The carrier densities of some 10^{13} cm^{-2} predicted theoretically are very high, however, the long lifetimes at low densities admit to generate such densities even under moderate optical excitation. Preliminary measurements indicate a quite complex screening dynamics including contributions from higher subbands in the PL signal that deserves further investigations. This concerns also the role of localized states ignored in the theoretical treatment.

The authors acknowledge support from PROFit program.

*fh@physik.hu-berlin.de

[1] S. Shigemori, A. Nakamura, J. Ishihara, T. Aoki, and J. Temmyo, Jpn. J. Appl. Phys., Part 2 **43**, L1088 (2004).
[2] S. Sadofev, S. Blumstengel, J. Cui, J. Puls, S. Rogaschewski, P. Schäfer, and F. Henneberger, Appl. Phys. Lett. **89**, 201907 (2006).
[3] S. Sadofev, P. Schäfer, Y.-H. Fan, S. Blumstengel, F. Henneberger, D. Schulz, and D. Klimm, Appl. Phys. Lett. **91**, 231103 (2007).
[4] S. Sadofev, S. Kalusniak, J. Puls, P. Schäfer, S. Blumstengel, and F. Henneberger, Appl. Phys. Lett. **91**, 231103 (2007).
[5] F. Bernardini, V. Fiorentini, and D. Vanderbilt, Phys. Rev. B **56**, R10024 (1997).
[6] S. F. Chichibu, A. C. Abare, M. S. Minsky, S. Keller, S. B. Fleischer, J. E. Bowers, E. Hu, U. K. Mishra, L. A. Coldren, S. P. DenBaars, and T. Sota, Appl. Phys. Lett. **73**, 2006 (1998).
[7] J. S. Im, H. Kollmer, J. Off, A. Sohmer, F. Scholz, and A. Hangleiter, Phys. Rev. B **57**, R9435 (1998).
[8] P. Lefebvre, A. Morel, M. Gallart, T. Taliercio, J. Allègre, B. Gil, H. Mathieu, B. Damilano, N. Grandjean, and J. Massies, Appl. Phys. Lett. **78**, 1252 (2001).
[9] P. Gopal and N. A. Spaldin, J. Electron. Mater. **35**, 538 (2006).
[10] C. Morhain, T. Bretagnon, P. Lefebvre, X. Tang, P. Valvin, T. Guillet, B. Gil, T. Taliercio, M. Teisseire-Doninelli, B. Vinter, and C. Deparis, Phys. Rev. B **72**, 241305(R) (2005).
[11] T. Makino, Y. Segawa, M. Kawasaki, A. Ohtomo, R. Shiroki, K. Tamura, and T. Yasuda, Appl. Phys. Lett. **78**, 1237 (2001).
[12] X. J. Wang, I. A. Buyanova, W. M. Chen, M. Izadifard, S. Rawal, D. P. Norton, S. J. Pearton, A. Osinsky, J. W. Dong, and Amir Dabiran, Appl. Phys. Lett. **89**, 151909 (2006).
[13] Jau-Jiun Chen, F. Ren, Yuanjie Li, D. P. Norton, S. J. Pearton, A. Osinsky, J. W. Dong, P. P. Chow, and J. F. Weaver, Appl. Phys. Lett. **87**, 192106 (2005).